

Phytoplankton community responses to the light spectrum gradient in the Baltic Sea

Elizabeth Sands^{1,2,*}, Bengt Karlson³, Anders F. Andersson⁴, Krzysztof T. Jurdzinski⁴, Ulf Båmstedt², Agneta Andersson^{1,2}

Abstract

Phytoplankton depend on light, and while intensity effects are well known, responses to light spectrum are less studied. The northern Baltic Sea appears increasingly brown due to CDOM, which absorbs blue light. Using incubation experiments and DNA barcoding on communities from Kattegat, the Central Baltic, and the Bothnian Bay, we show that browner, red-shifted light promotes mixotrophs and heterotrophs. Green algae from the Bothnian Bay tolerated red light, unlike those from southern regions, indicating local adaptation. These results reveal CDOM-driven spectral selection shaping northern Baltic phytoplankton communities as browning intensifies.

Keywords

Phytoplankton; Metabarcoding; Community; Baltic Sea; CDOM; Light spectra; Green algae, Trophic

¹Department of Ecology and Environmental Science, 901 76 Umeå University, Umeå, Sweden

²Umeå Marine Science Centre, Umeå University, 905 71 Hörnefors, Umeå, Sweden

³Research and Development, Oceanography, Swedish Meteorological and Hydrological Institute, Göteborgsgeskaderns plats 3, 426 71, Västra Frölunda, Gothenburg, Sweden

⁴KTH Royal Institute of Technology, Department of Gene Technology, Science for Life Laboratory, Stockholm, Sweden

*Correspondence: elizabeth.sands@umu.se (E. Sands)

Received: 18 November 2025; revised: 16 March 2026; accepted: 18 June 2026

1. Introduction

Light intensity is a key driver of phytoplankton adaptation. Species that efficiently utilise photosynthetically available radiation (PAR) have a competitive advantage in their environment (Demir-Hilton et al., 2011; Edwards, Litchman and Klausmeier, 2013). Less is known about responses to spectral quality of the light environment, which can also affect species distribution and support functional diversity. Knowledge of the underwater light spectra compared to primary production and the absorption spectra of phytoplankton have been used to improve remote sensing (Sakshaug and Slagstad, 1991; Johnsen et al., 1992; Werdell et al., 2018). The visible light which enters the marine environment is subject to absorption by water, this causes the longer wavelengths of red and green to be increasingly lost with depth so that oligotrophic oceans appear blue. Other light-absorbing constituents of ocean water, such as chromophoric/coloured dissolved organic matter (CDOM) and phytoplankton, can vary in their relative contributions and overlap in their effect on the light spectrum (Allen et al., 2020). For this reason, the Baltic Sea, which is greatly influ-

enced by terrestrial CDOM, is classed as optically complex (Levin et al., 2013).

The environmental gradients in the Baltic Sea make it a useful model to forecast effects of change in marine systems. In this semi-enclosed sea, there are north-south gradients of decreasing CDOM, increased temperature and salinity, and the limiting nutrient shifts from phosphorus to nitrogen. CDOM primarily absorbs light in the blue part of the spectrum so that light in waters of the northern Baltic is shifted towards red wavelengths which gives it a brown appearance (Harvey et al., 2015; Simis et al., 2017; Kratzer and Moore, 2018). Terrestrial CDOM runs off from soils after rainfall and drains into the Baltic. Studies of boreal lakes point to land use and afforestation, iron deposition, and reduced sulphur input from acid rain as causes of an increase in CDOM (Xiao et al., 2020; Škerlep et al., 2022). Rainfall and CDOM levels are projected to increase further with climate change and this has implications for the survival, proliferation, and the composition of future phytoplankton communities (Paczkowska et al., 2017; Strååt, Mörth and Undeman, 2018). Terrestrial CDOM addition can alter the food web by promoting heterotrophic bacteria and mixotrophic phytoplankton over phototrophs (Båmstedt and Wikner, 2016; Figueroa et al., 2016; Spilling et al.,

2022). This is likely because waters subject to browning have both a reduced intensity and a narrower spectrum of light available for photosynthesis.

Chlorophylls and other pigments that phytoplankton use to capture light have absorbance peaks at different wavelengths. The combination of these pigments is species-specific and can also be adjusted dynamically. For example, *Synechococcus* spp. cyanobacteria exploit spectral niches by adjusting cellular contents of red/orange wavelength absorbing phycocyanin and blue/green absorbing phycoerythrin pigments (Kehoe and Grossman, 1994; Palenik, 2001; Stomp et al., 2004). Picocyanobacteria in the Baltic show diversity in phycocyanin operon sequence, suggesting specialisation to the light environment (Haverkamp et al., 2009; Larsson et al., 2014). Cyanobacteria outcompete eukaryotes in competition experiments in green light (Luimstra et al., 2020). Green algae and most other eukaryotic phytoplankton exhibit higher growth rates in blue light (Neun et al., 2022). Some eukaryotic phytoplankton show adaptations to light environments. For example, the green alga, *Ostreococcus*, associated with oligotrophic ocean waters responds to red, green, and blue light distinctly at transcriptional and physiological levels (Sands et al., 2023). The diatom *Phaeodactylum tricornutum* also exhibits distinct transcriptional responses to red, green, and blue light (Valle et al., 2014; Fortunato et al., 2016). These examples demonstrate a precedent for light quality responses in phytoplankton, suggesting that the ability to discern and respond to specific wavelengths is advantageous. Most of these studies have, however, been performed using isolates, which calls for investigations in natural habitats.

In this study we seek to determine whether the brown light environment contributes to the phytoplankton community structure changes seen along the north-south gradient of the Baltic Sea and to the Kattegat, an area of transition to the North Sea (Wasmund and Uhlig, 2003; Paczkowska et al., 2017). We hypothesise that phytoplankton in the Northern Baltic are adapted to browning light. These adaptations may confer competitive advantages to certain taxa and thereby influence community composition. In the applied nutrient replete conditions, and the reduced light spectra in this experiment, we expected a shift favouring heterotrophic and mixotrophic plankton in the red and brown treatments. For efficient light capture in the narrowed spectrum of brown light, we expected that dominating species would be those which produce high levels of chlorophyll *a* (Chl-*a*), phycoerythrin, and phycocyanin. To test this hypothesis, we conducted controlled competition experiments under different spectral treatments to identify which light conditions favour specific phytoplankton taxa and whether taxa from different sites respond differently.

Seawater samples were taken from sites along the Baltic Sea gradient and incubated under three light spectra at equal PAR; a blue and green enriched spectrum broadly

characteristic of oligotrophic marine waters (Stomp et al., 2007), an orange/brown spectrum representing increased absorption of short wavelengths typical of CDOM rich waters, and an extreme treatment of red wavelengths only. The samples were incubated for 10 days to allow development of different phytoplankton groups/taxa in the light spectra. Phytoplankton groups were analysed using 16S and 18S metabarcoding.

2. Methods

Seawater samples were collected in a CDOM gradient in Swedish marine waters during autumn 2022. The following physicochemical parameters at the sites were collected as part of ongoing monitoring and accessed on SHARK-Web (SMHI, 2023). Humic substances were detected by fluorescence at 350/450 nm. DOC was detected by high-temperature combustion with non-dispersive infrared absorption (NDIR). Further details of monitoring data collection are given with Supplementary Table 1.

Data on light absorption at 412 nm were obtained from the Aqua MODIS Level 3 dataset on NASA Ocean Color at a 4 km resolution (Modis, 2022) as in Hill et al. (2019), and displayed using ArcGIS. This data was used to provide a regional overview of spatial differences in humic content across the Baltic Sea, although uncertainties remain for absolute concentrations in optically complex coastal waters.

2.1 Field sampling

Three stations with depths of 50 to 100 m were selected, Supplementary Table 1. Sampling was carried out on the r/v *Svea* in September 2022 for the Kattegat (Anholt E, Lat. 56.66783, Long. 12.112) and the Gotland Basin station, Central Baltic Proper (BY39, Lat. 56.11600, Long. 16.53433) stations, and on the vessel *KBV181* in October 2022 for the Bothnian Bay Station (F3/A5, Lat. 65.16633, Long 23.23283) (Figure 1). Stations were sampled during daylight. Based on 1% surface irradiance depths ranging from 3.2 to 15.4 m in the northern Bothnian Bay (Båmstedt and Wikner, 2016), a 2 m depth was selected for light measurements, sample collection, and experimental light conditions. Relative irradiance across the visible spectrum was measured at a depth of 2 m (unshaded side of vessel) using an OceanInsight Spectrometer USB4000 calibrated using a halogen lamp (Ocean Optics™ calibration unit, HAL 2000) (Båmstedt, 2019) and analysed using OceanView software 2.0.14 (Figure 2). The fibre-optical cable was aimed vertically up towards the surface to capture downwelling irradiation.

Water was collected from a depth of 2 m, using CTD bottles. On board the ship, the water was stored at 12°C and exposed to shaded daylight for around 4 to 5 hrs per day to allow survival with minimal growth. The transport time from sampling to the laboratory spanned between 30 hours and 6 days, and in each case, experimentation was

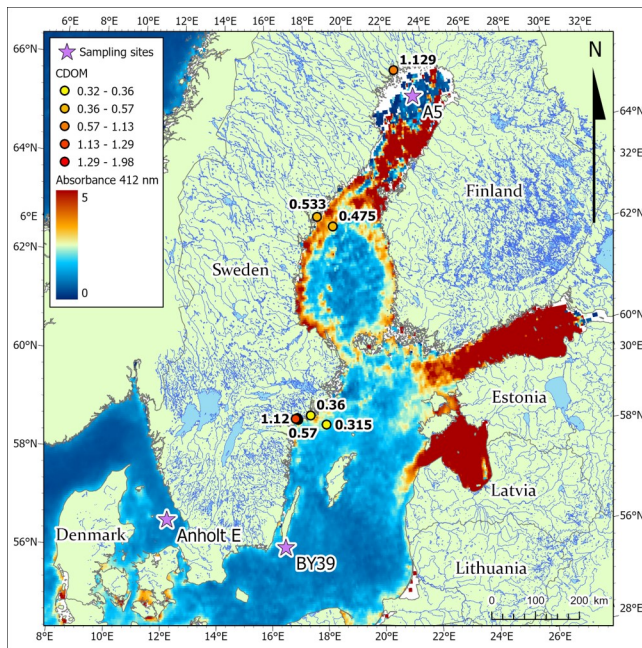


Figure 1. Sampling sites and mean absorbance at 412 nm for September 2022, overlaid in circles with measurements of CDOM at a 1 m depth by absorption (g_{440}) estimate m^{-1} from monitoring surveys at a limited number of sites. Data from MODIS Aqua by NASA Ocean Color (Modis, 2022) and SHARKWeb (SMHI, 2023). Length 17 cm.

carried out immediately on arrival of samples to the lab on land.

Three replicates of 500 ml water were vacuum filtered (20kPa) onto 0.2 μm filters (Pall Acrodisc™ Syringe Filters with Supor™ Membrane, Sterile, 32 mm) at time of water collection and stored at $-20^{\circ}C$ in 700 μl DNA Shield (Zymo Research) for later DNA extraction.

2.2 Incubation experiment

After transport to the onshore lab and immediately prior to incubation, three further replicates of 500 ml water from each site were vacuum filtered for metabarcoding. These samples were used to check for loss of taxa during transport and are referred to as the lab community.

The samples were subjected to three spectral light regimes: blue/green light, orange/brown light, and red light. For the blue and green treatment, 77% of total irradiance measured was blue wavelengths between 400–499 nm. In the browning spectrum, 53% of irradiance measured was in the green range between 500–599 nm, and 30% in the red between 600 and 699 nm. The red treatment had 94% irradiance in the red range, 600–699 nm. The spectra were formed by filters over fluorescent light-bulbs (Supplementary Figure 1) and the samples were incubated at $12^{\circ}C$ in a regime of 8 hours darkness, 16 hours light. Samples of 500 ml were placed into cell culture flasks with vented filter caps (T175, Sarstedt Inc.) as 3 replicates

in each of the 3 light treatments. Flasks were set to receive 4 μmol photons $m^{-2} s^{-1}$ light 400–700 nm using a Walz PAR meter with a flat sensor. This low light was to ensure limitation. This light level is relevant and sufficient for photosynthesis of Baltic phytoplankton, Supplementary Table 2 (Andersson et al., 1989; Ask et al., 2016; Biggs et al., 2022). To prevent nutrient limitation, Guillard's (F/2) Marine Water Enrichment Solution with silica was used. The flasks were incubated standing upright for 10 days with twice daily gentle mixing by inversion and samples were vacuum filtered as before.

2.3 Metabarcoding of 16S and 18S RNA genes

All samples were stored at $-80^{\circ}C$ prior to DNA extraction using ZymoBIOMICS DNA/RNA Miniprep Kit (Ver. 2.0.0). Amplification of 16S gene was performed by PCR using the Nanopore (SQK-16S024) kit and the standard protocol. The kit amplifies full-length 16S using the primers 27F 5'-AGAGTTTGATCMTGGCTCAG and 1492R 5'-CGGTACCTTGTACGACTT. 4 ng DNA per sample were pooled for a total of 88 ng per library for sequencing. Amplification of 18S gene was carried out twice using two sets of primers to amplify two variable regions. Balzano primers amplify the V4 region: V4F CCAGCASCYCGGTAATTCC and V4RB ACTTTCGTTCTTGATYRR (Balzano et al., 2015; Latz et al., 2022), and Hugerth primers amplify the V9 region 574*F CGGTAAYTCCAGCTCYAV and 1132R CCGTCAATTHCTTYAART (Hugerth et al., 2014). LongAmp™ Hot Start Taq from New England BioLabs was used to amplify the 18S gene, as this gives fragments with dA-tails at the 3' ends. Bovine serum albumen was used to bind inhibitors. The ligation kit SQK-LSK109 from Oxford Nanopore was used to ligate adapters. Full PCR conditions can be found in the supplementary information. Sequencing of both 16S and 18S was carried out using Nanopore MinION technology and flow cells type FLO-MIN106 (Oxford Nanopore Technologies plc).

2.3.1 Downstream sequencing analysis pipeline

For the downstream analyses, MinKNOW software version 23.07.12 with Dorado 7.1.4 (c) 2023 Oxford Nanopore Technologies PLC was used to basecall reads in 450 bps HAC mode (high accuracy). For the 18S datasets, samples were demultiplexed and barcode indexes, adapters, and primers trimmed with MiniBar.py version 0.24 (Krehenwinkel et al., 2019) which recognises different forward and reverse barcode index sequences. Read quality and length were assessed using NanoPlot V1.4.1.6 (De Coster and Rademakers, 2023). Reads were trimmed using Chopper v0.6.0 (De Coster and Rademakers, 2023). Min length 200, max 700 for 18S Balzano gave a mean quality of Q13.8. Min length 200, max 900 for 18S Hugerth gave a mean of Q13.4. Min length 200, max 2000 for 16S gave a mean of Q13.6.

To identify taxa and their relative abundances in each sample, QIIME2 (version amplicon-2023.9) was used to

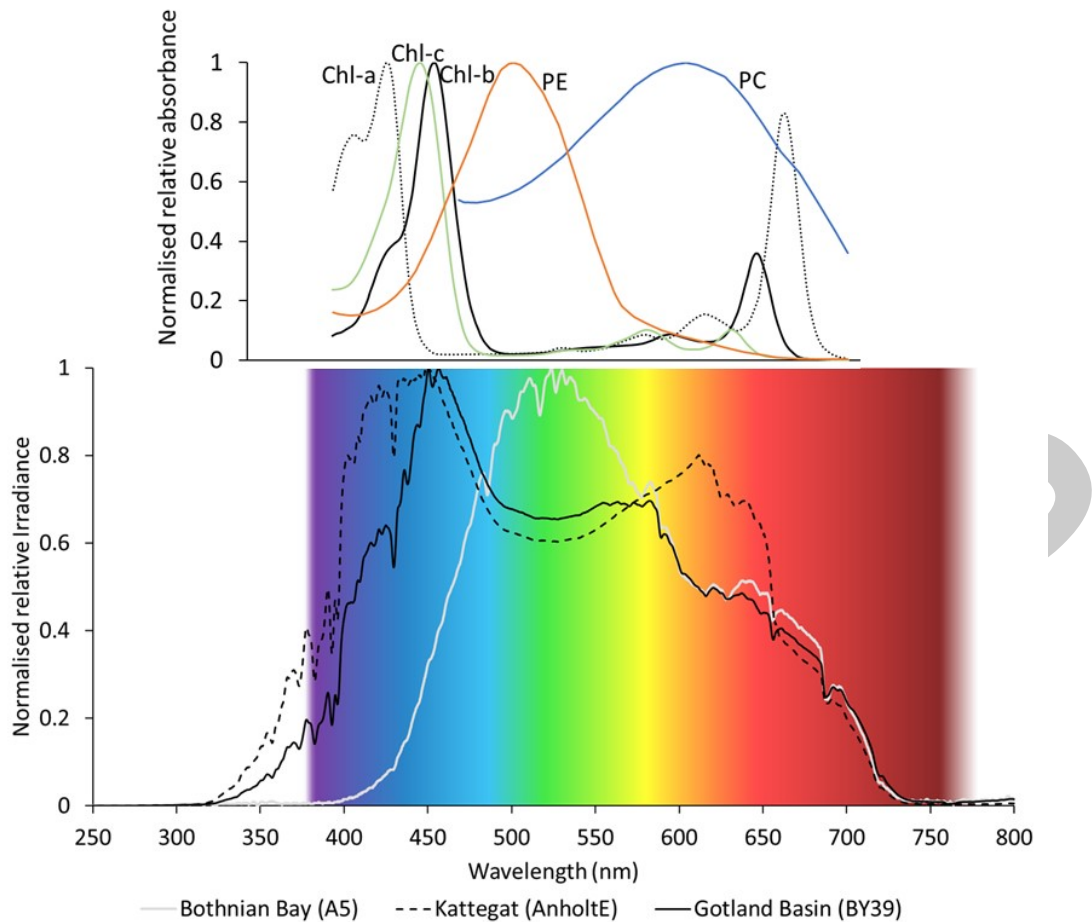


Figure 2. Relative irradiance of light wavelengths at a 2 m depth normalised to maximum irradiance. Absorbance spectra of key algal chlorophylls and pigments from the PhotochemCAD database (Taniguchi and Lindsey, 2023).

234 perform closed reference clustering by VSearch at 97%
 235 identity to form OTUs (Operational Taxonomic Units)
 236 (Rognes et al., 2016; Bokulich et al., 2018; Bolyen et al.,
 237 2019). This method permits clustering regardless of taxon-
 238 omic level, but is limited to the database used, and allows
 239 direct comparison of the two 18S primer sets. The same
 240 databases were used for clustering and taxonomy. Fea-
 241 tures of less than ten occurrences across all samples were
 242 removed. Tools for Nanopore data only provide OTUs via
 243 clustering as denoising is not designed to handle this data
 244 (Santos et al., 2020). Taxonomy for 18S reads was assigned
 245 with PR2 database 5.0.0 (Guillou et al., 2013), identify-
 246 ing 123 named OTUs in the Hugerth primer dataset, and
 247 207 OTUs in the Balzano dataset. Taxonomy for 16S reads
 248 was assigned using Greengenes 2022.10 (McDonald et al.,
 249 2023) which identified 343 OTUs.

250 2.4 Differential abundance of taxonomic groups

251 For the following analyses, Metazoa were removed. ANCOM-
 252 BC (analysis of composition with bias correction using
 253 linear regression) was used to test for significantly differ-
 254 ential abundances of taxa (Lin and Peddada, 2020). Taxa

255 were also grouped according to trophic types assigned by
 256 SMHI (SMHI, 2023) and (Olenina et al., 2006) and similarly
 257 to studies of lake browning (Senar et al., 2021). Eukaryotic
 258 taxa were grouped into: green algae, diatoms, other
 259 phototrophs, mixotrophs, and heterotrophs. Phototrophic
 260 and mixotrophic taxa were then grouped by major photo-
 261 synthetic pigments (other than chlorophyll *a*) (Roy et
 262 al., 2011). The three groups were: chlorophyll *b* (Chl-*b*),
 263 chlorophyll *c* (Chl-*c*), and both chlorophyll *c* and phyco-
 264 biliproteins (Chl-*c* PB). 16S taxa were also grouped accord-
 265 ing to photosynthetic potential into alphaproteobacteria,
 266 gammaproteobacteria, other heterotrophs, and cyanobac-
 267 teria (excluding Vampirovibrionia which are heterotrophs).
 268 Taxa assigned to these groupings are given in Supplemen-
 269 tary Table 3. ANOVA and post hoc Tukey's HSD tests were
 270 used to test for significant differences in relative abun-
 271 dances of the trophic and pigment groupings.

272 The two primers used for the 18S amplicons, Hugerth
 273 and Balzano, gave similar results for dominant and signifi-
 274 cant taxa (Supplementary Figure 3). The results presented
 275 are from the Balzano primers as this was of a greater depth
 276 and gave more named OTUs.

3. Results

3.1 Physicochemical characteristics of sample sites

Weather conditions were similar at all stations, with sunny and calm seas. The following monitoring data was accessed on SHARKWeb (SMHI, 2023). Chlorophyll *a* concentrations were similar at all stations, $\sim 2\text{--}3\ \mu\text{g/L}$. The water temperature was $15\text{--}16^\circ\text{C}$ in the Kattegat (Anholt E) and Gotland Basin (BY39) stations and around 9°C in the Bothnian Bay (F3/A5) station. Total nitrogen and silicate increased from south to north, while total phosphorus was lowest in the Bothnian Bay. The Secchi depth was greater in the Kattegat (9 m) than in the Bothnian Bay (5 m), Supplementary Table 1.

The concentration of humic substances at the Bothnian Bay site was $20.1\ \mu\text{g/L}$, 5-fold higher than in the Kattegat, $4.1\ \mu\text{g/L}$. In line with this, September–October measurements from 2012 to 2022 show means of $16.9\ \mu\text{g/L}$ at the Bothnian Bay station and $4.4\ \mu\text{g/L}$ at the Kattegat station. Dissolved organic carbon (DOC) at the Bothnian Bay station was $405\ \mu\text{mol/L}$ at a depth of 5 m (mean of $377\ \mu\text{mol/L}$ for September and October readings 2013 to 2022). CDOM in the Bothnian Bay station had a mean absorption (g_{440})

estimate of $0.9\ \text{m}^{-1}$ between surface and 1 m depth for Septembers 2018 to 2022, also from monitoring data on SHARKWeb, (SMHI, 2023). For the two southern sites, absorbance at 412 nm was detected remotely by MODIS Aqua, NASA Ocean Color (Modis, 2022). Means of these data have been plotted for September 2022 alongside measurements of CDOM at a 1 m depth in absorption (g_{440}) estimate m^{-1} during monitoring surveys at limited sites as on SHARKWeb (SMHI, 2023) (Figure 1). Further absorbance estimations at 412 nm using MODIS data covering monthly means for 2022, annual means for 2013–2022, and September means for 2013–2022 (Supplementary Figures 5a–c).

3.2 Spectral characteristics vary by site

An initial depth profile at the Bothnian Bay site had shown that the spectrum is narrowed considerably by a depth of 2 m and the overall irradiance is also reduced (Supplementary Figure 3). This was also seen in our measurements during sampling (Figure 2). Blue wavelengths were greatly reduced below 450 nm, while green through to red wavelengths remained relatively prominent. In contrast, at both southerly sites, a greater irradiance of light

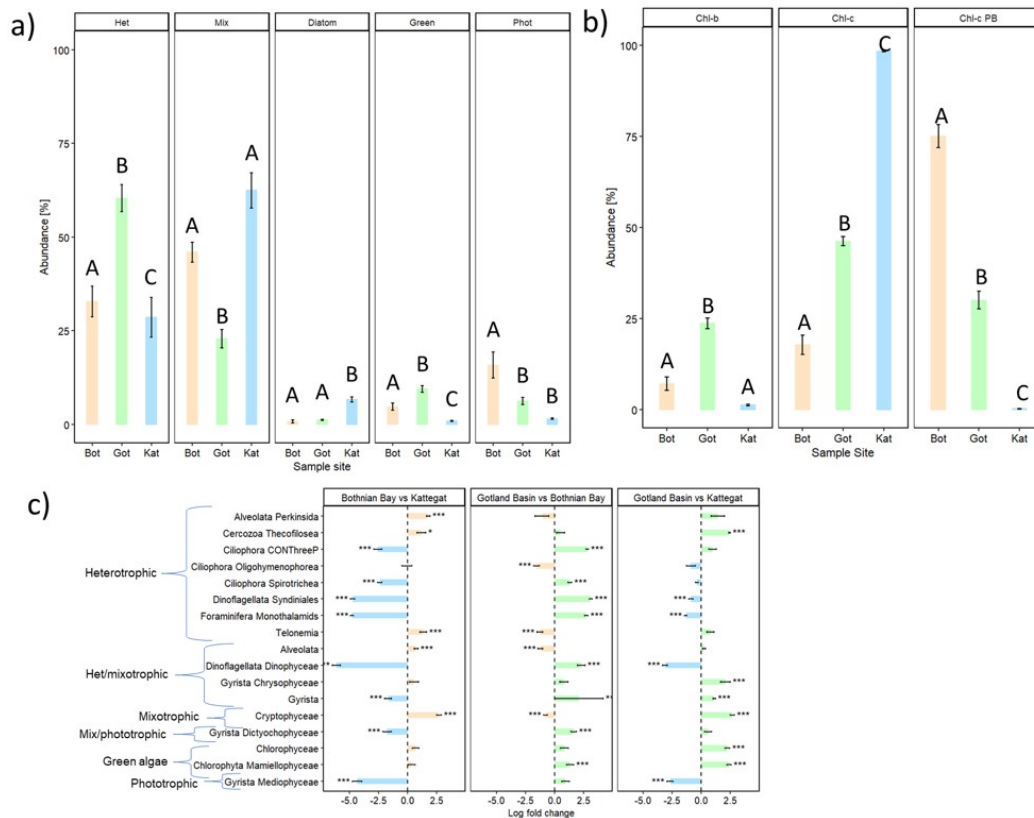


Figure 3. Eukaryotic taxa relative abundances at sites at the time of sampling. Percentages exclude unknown OTUs, Metazoa, and those unassigned to groupings. Taxa grouped by trophic mode (a), phototrophic and mixotrophic taxa grouped by major photosynthetic pigment (b), taxa which differed significantly among sites as identified by ANCOM-BC analysis (c). Data are means and standard errors. Different letters indicate significant differences ($P < 0.05$) determined by Tukey's test.

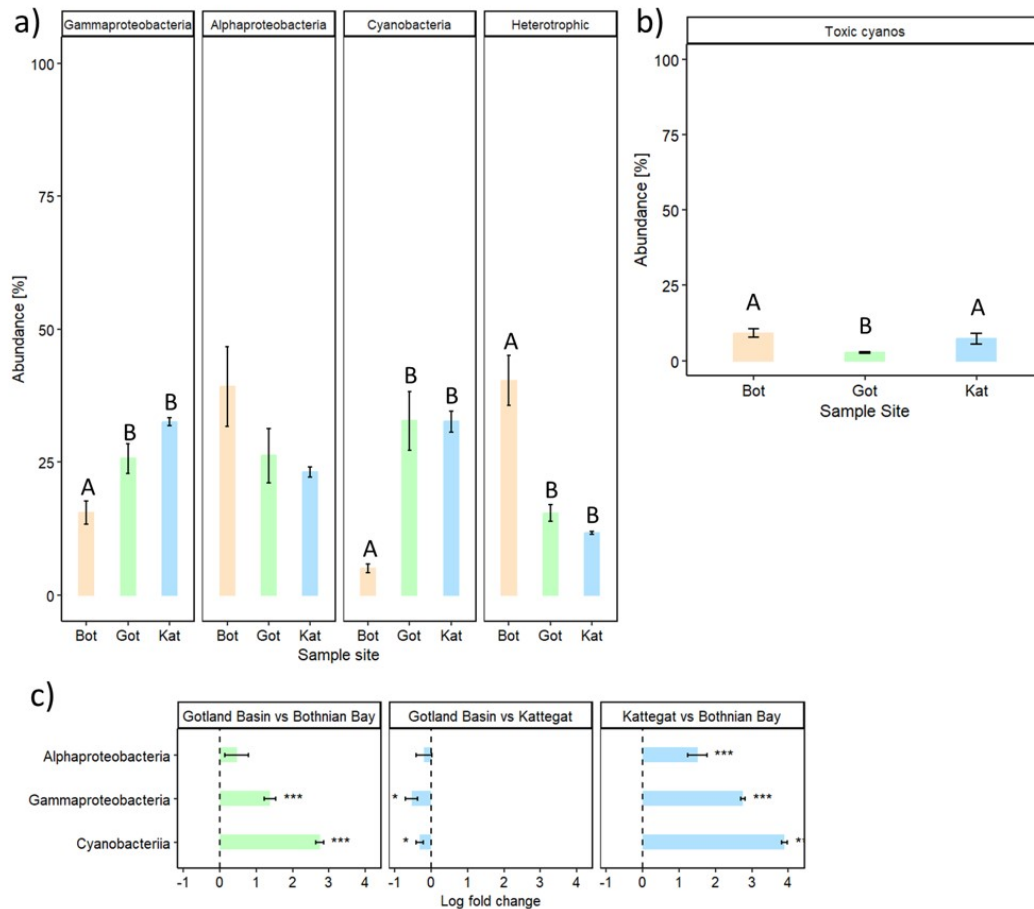


Figure 4. Relative abundances of bacterial taxa at sites. Taxa grouped by photosynthetic potential (a), percentage of cyanobacteria which are potentially toxic (b), taxa which differed significantly between sites as identified by ANCOM-BC analysis (c). Data are means and standard errors. Different letters indicate significant differences ($P < 0.05$) determined by Tukey's test.

was present across the visible spectrum at this shallow reading. UV light was reduced at all sites and was not present in the Bothnian Bay reading. A comparison of light colour by percentage of total PAR irradiance was made, wavelengths were grouped into: 400–499 nm for blue, 500–599 nm for green, and 600 to 799 nm for red. This showed that the Bothnian Bay differs from the southerly sites with lower proportions of blue (22% of the total PAR versus 40% in the other sites) and higher proportions of green wavelengths (51% versus 37% and 32% in the Gotland Basin and Kattegat sites respectively). The total PAR was also much lower overall in the Bothnian Bay site, (Supplementary Figure 1b). The green light proportion was also slightly elevated in Gotland Basin compared to the Kattegat site.

3.3 Community structure and composition across sites

The proportions of taxa in the communities were different at each site. The Bothnian Bay had significantly higher proportions of mixotrophic cryptophyte OTUs than other

sites (mean relative abundance of 50% versus 12% and 0.2% for Gotland Basin and Kattegat respectively), and more chlorophytes than the Kattegat (5% versus 0.4%) (Figure 3c). The Kattegat samples had the highest proportions of dinoflagellates (68% mostly *Syndiniales* and *Dinophyceae*, versus 15% and 1.4% in the Gotland Basin and Bothnian Bay) and diatoms (7% mostly *Mediophyceae* versus 2.8% and 1.7% in the Gotland Basin and Bothnian Bay).

Eukaryotic taxa were grouped according to taxonomic and trophic types. When comparing the relative proportions of taxa in these groups, the Gotland Basin site had the most heterotrophs, and the least mixotrophs. The Kattegat site had the most diatoms and the least green algae, and the Bothnian Bay site had the highest proportion of other phototrophs (Figure 3a). Phototrophic and mixotrophs were then grouped by major photosynthetic pigment (other than chlorophyll *a*) according to taxonomy. The three groups were: chlorophyll *b* (Chl-*b*), chlorophyll *c* (Chl-*c*), and both chlorophyll *c* and phycobiliproteins (Chl-*c* PB). The Gotland

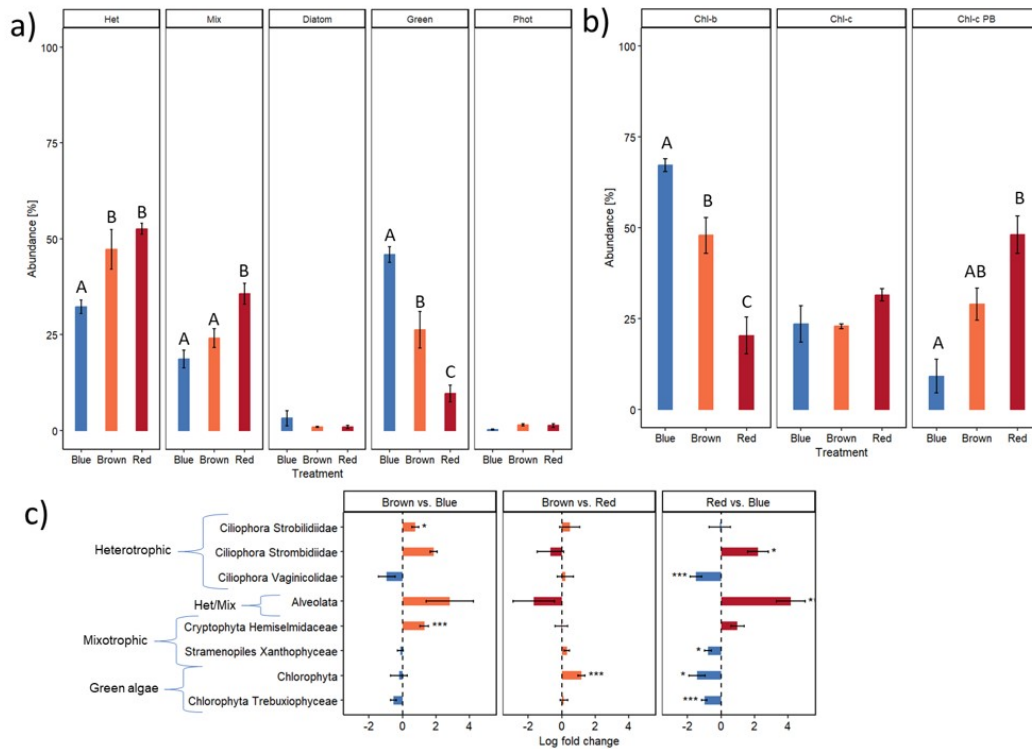


Figure 5. Relative abundances of eukaryotic taxa for the Bothnian Bay after light incubation. Percentages exclude unknown OTUs, Metazoa, and unassigned groupings. Taxa grouped by trophic mode (a), phototrophic and mixotrophic taxa grouped by major photosynthetic pigment (b), taxa which differed significantly after incubation as identified by ANCOM-BC analysis (c). Data are means and standard errors. Different letters indicate significant differences ($P < 0.05$) determined by Tukey's test.

Basin site had the highest proportion of Chl-*b* containing taxa. The Kattegat site had the most Chl-*c* containing taxa, this is explained by the higher proportions of diatoms and dinoflagellates. The Bothnian Bay had the highest proportion of Chl-*c* PB containing taxa (Figure 3b).

From the 16S amplicon data, the Bothnian Bay site had the lowest proportion of cyanobacteria (5% versus 32% for both Gotland Basin and Kattegat sites) and gammaproteobacteria (16% versus 26% and 33%). The Bothnian Bay had the highest proportions of alphaproteobacteria (40% versus 27% and 23% in the Gotland Basin and Kattegat sites) and other heterotrophic bacteria (40% versus 15% and 12%). Proportions of the total cyanobacteria which are considered toxic or able to form HABs (harmful algal blooms) were compared across sites, taxa listed in Supplementary Table 4. These were low overall but showed higher relative abundances in the Bothnian Bay (9%) and Kattegat (7%) sites at the point of sampling compared to the Gotland Basin (3%) (Figure 4b).

3.4 Community structure comparisons among light treatments

3.4.1 Bothnian Bay

All light treated samples diverged from the initial lab community to a similar extent, (Supplementary Figure 5), how-

ever eukaryotic communities grown in brown light diverged least.

Blue light favoured chlorophyte green algae (mainly *Bathycoccus* spp.) which reached 46% of the community (Figure 5a). The blue light samples therefore had the highest proportion of taxa which use Chl-*b* (Figure 5b). Other phototrophs and heterotrophs were comparatively lower in blue, as were cryptophytes (at 6%) and Alveolata (including Ciliophora) (at 8%).

In the bacterial community, cyanobacteria proportions were low in blue light (2%), while Gammaproteobacteria accounted for 58% (Figure 6a,c). Alphaproteobacteria remained ~21%.

Under brown light, chlorophyte proportions were intermediate between blue and red treatments. Mixotrophic Cryptophyta increased to 15%, and heterotroph proportions were higher than in blue light. Alveolata remained low in brown light (13%). Cyanobacteria proportions remained at 2%, and Gammaproteobacteria were similar to blue light. Alphaproteobacteria proportions did not differ significantly (~21%).

Red light reduced chlorophyte relative abundance to 10% (Figure 5a). In contrast, other phototrophs and mixotrophs increased, with Cryptophyta reaching 23%.

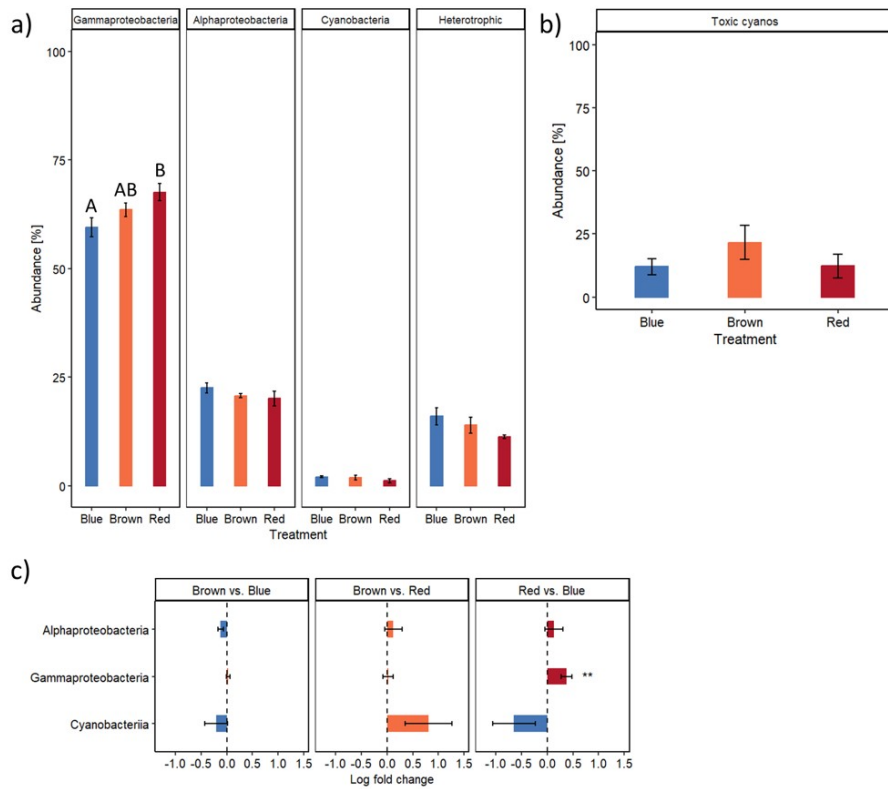


Figure 6. Relative abundances of eukaryotic taxa for the Bothnian Bay after light incubation. Percentages exclude unknown OTUs, Metazoa, and unassigned groupings. Taxa grouped by trophic mode (a), phototrophic and mixotrophic taxa grouped by major photosynthetic pigment (b), taxa which differed significantly after incubation as identified by ANCOM-BC analysis (c). Data are means and standard errors. Different letters indicate significant differences ($P < 0.05$) determined by Tukey's test.

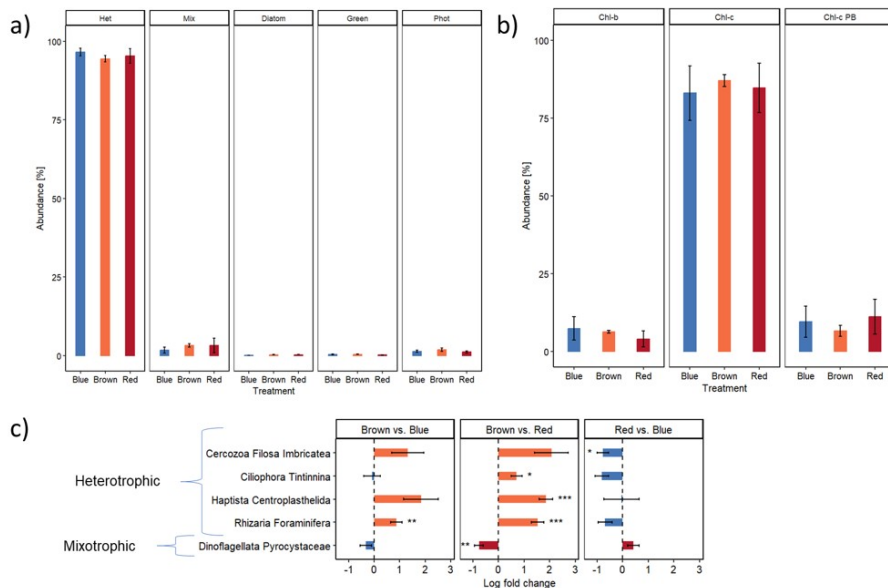


Figure 7. Relative abundances of eukaryotic taxa for samples from the Gotland Basin after light incubation. Percentages exclude unknown OTUs, Metazoa, and those which could not be assigned to groupings. Taxa grouped by trophic mode (a), phototrophic and mixotrophic taxa grouped by major photosynthetic pigment (b), taxa which differed significantly after incubation as identified by ANCOM-BC analysis (c). Data are means and standard errors. No significant differences were seen between treatments for a) and b).

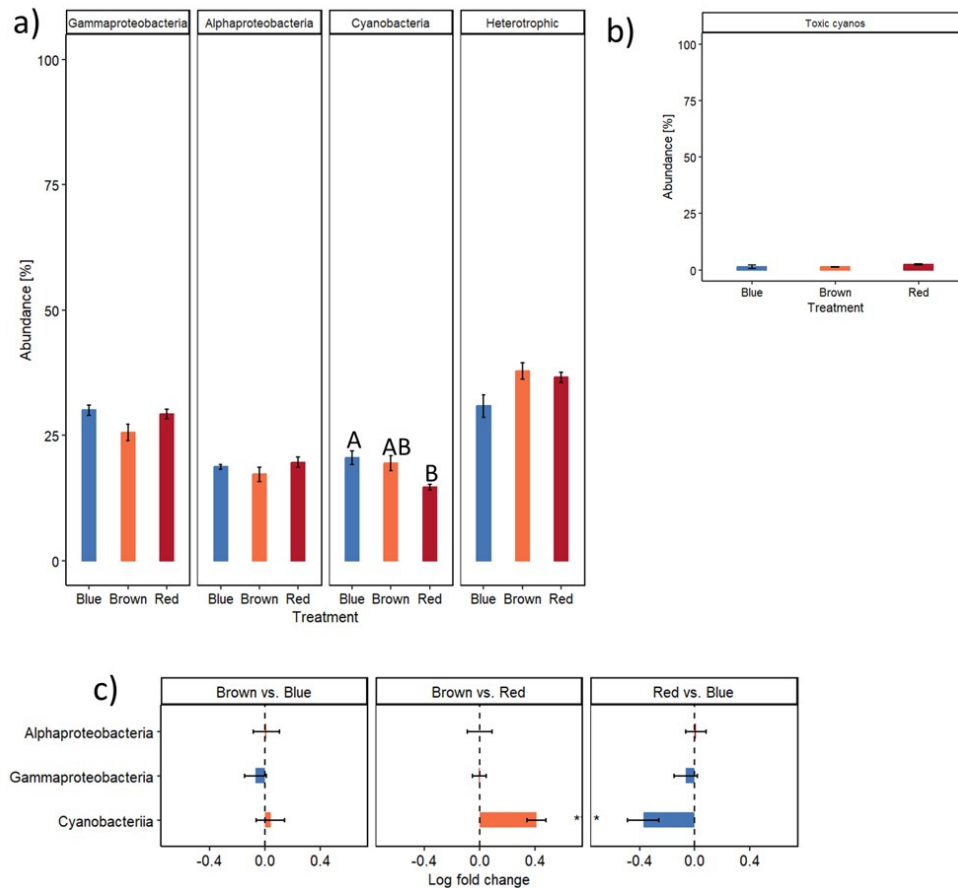


Figure 8. Relative abundances of bacterial taxa for samples from the Gotland Basin after light incubation. Taxa grouped by photosynthetic potential (a), percentage of cyanobacteria which are potentially toxic (b), taxa which differed significantly after incubation as identified by ANCOM-BC analysis (c). Data are means and standard errors. Different letters indicate significant differences ($P < 0.05$) determined by Tukey's test.

Alveolata proportions were highest in red light (18%) (Figure 5c). Red light treated communities also had higher proportions of heterotrophs than in blue light.

Taxa with Chl-*c* PB were relatively highest in red light (Figure 5b), whereas there were no significant changes in taxa possessing Chl-*c* alone. This suggests a switch in competitive advantage conferred by the light harvesting capabilities of these chlorophylls and pigments.

In bacterial communities, cyanobacteria proportions decreased slightly to 1% in red light (Figure 6a,c), while gammaproteobacteria proportions increased to 68%. Proportions of toxic cyanobacteria did not differ among the light treatments (Figure 6b).

3.4.2 Gotland Basin

A similar level of divergence from the starting community was seen in all treatments (Supplementary Figure 5). However, unlike the Bothnian Bay, light treatments did not produce marked shifts in trophic structure. Chlorophytes were low in all lights (0.2% to 0.3%) (Figure 7a). *Telonemia* (heterotrophic) proportions were generally large (16%

to 20%), and heterotrophy dominated at ~95%. Diatom and green algae proportions were particularly low after all treatments. No significant differences were observed in trophic type or accessory pigments among the light treated samples (Figure 7a–b). Of the phototrophs that were present, the major accessory pigment type was mainly of Chl-*c* at ~87%.

On comparison of the bacterial communities, cyanobacteria proportions were highest at 20% in blue, 19% in brown, and lower at 15% in red light. The cyanobiaceae proportions were 0.3% in all three light treatments. Gammaproteobacteria, alphaproteobacteria, other heterotrophic bacteria, and toxic cyanobacteria proportions did not vary significantly (Figure 8a–c).

3.4.3 Kattegat

All light treated samples diverged similarly, though red treated samples diverged most from the prior lab community (Supplementary Figure 5).

Blue light supported the highest combined diatom proportions and lower heterotrophic dominance relative to

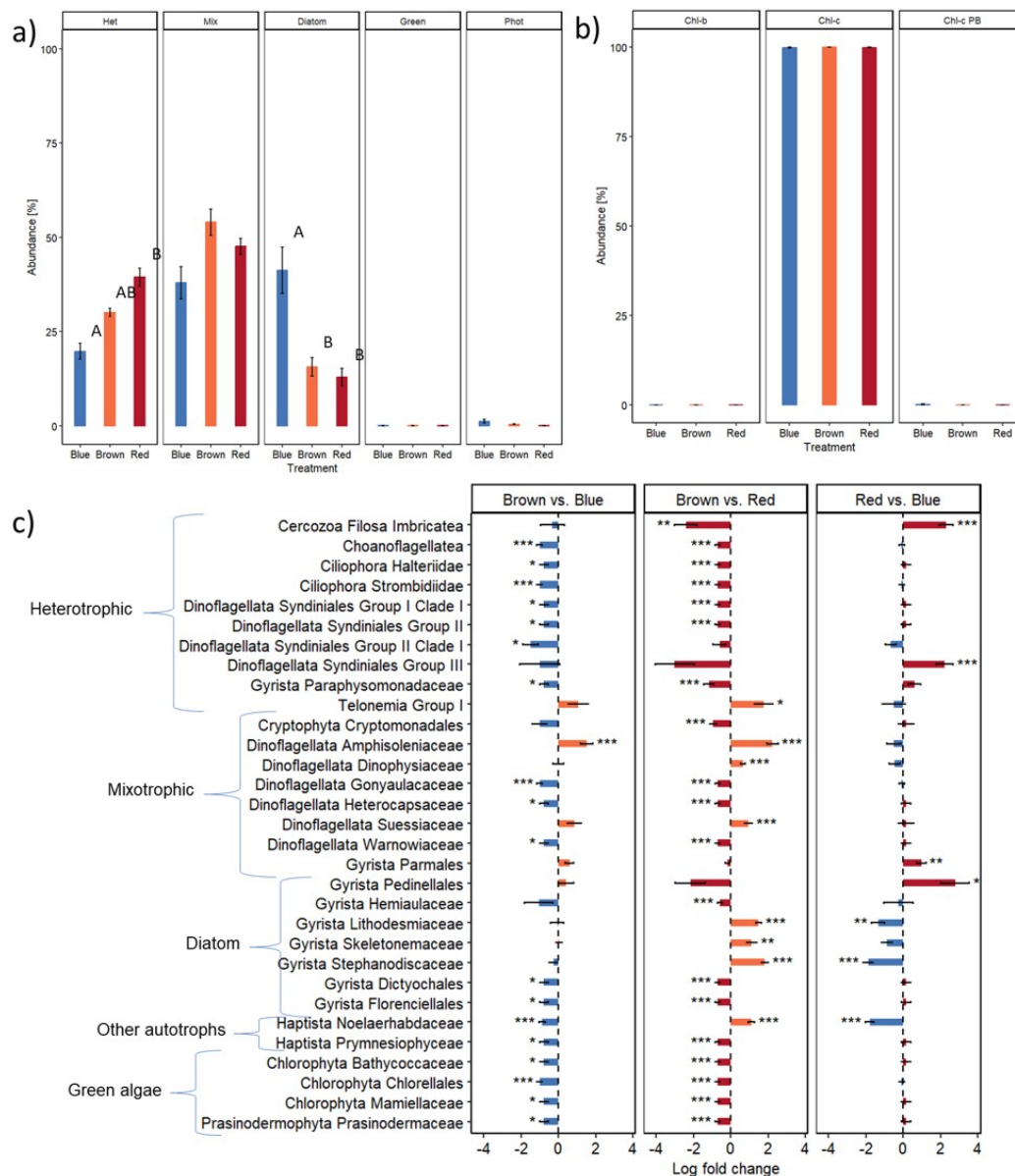


Figure 9. Relative abundances of eukaryotes from the Kattegat after light incubation. Percentages exclude unknown OTUs, Metazoa, and those unassigned to groupings. Taxa grouped by trophic mode (a), phototrophic and mixotrophic taxa grouped by major photosynthetic pigment (b), taxa which differed significantly after incubation as identified by ANCOM-BC analysis (c). Data are means and standard errors. Different letters indicate significant differences ($P < 0.05$) determined by Tukey's test.

red and brown treatments (Figure 9a). Total dinoflagellates were lowest in blue (44%). Cyanobacteria were highest in blue light (44%) (Figure 10a). Alphaproteobacteria were lowest in blue (18%).

Brown light increased *Telonemia* proportions (Figure 9c). Dinoflagellates increased to 58%. Phototrophs remained low overall. Cyanobacteria declined to 24%, and Alphaproteobacteria proportions were intermediate between blue and red treatments.

Red light further increased dinoflagellates (67%), in-

cluding *Syndiniales* Group III (parasites of other dinoflagellates), and increased the diatom group *Pedinellales*. Phototroph proportions remained low overall. Cyanobacteria proportions declined to 20%. Toxic cyanobacteria proportions were low overall but slightly higher in red than blue light. Alphaproteobacteria increased markedly to 38% in red light (Figure 10a-c). Toxic cyanobacteria proportions were low overall though higher in red light compared to blue.

As in the Gotland Basin, the dominant pigment category

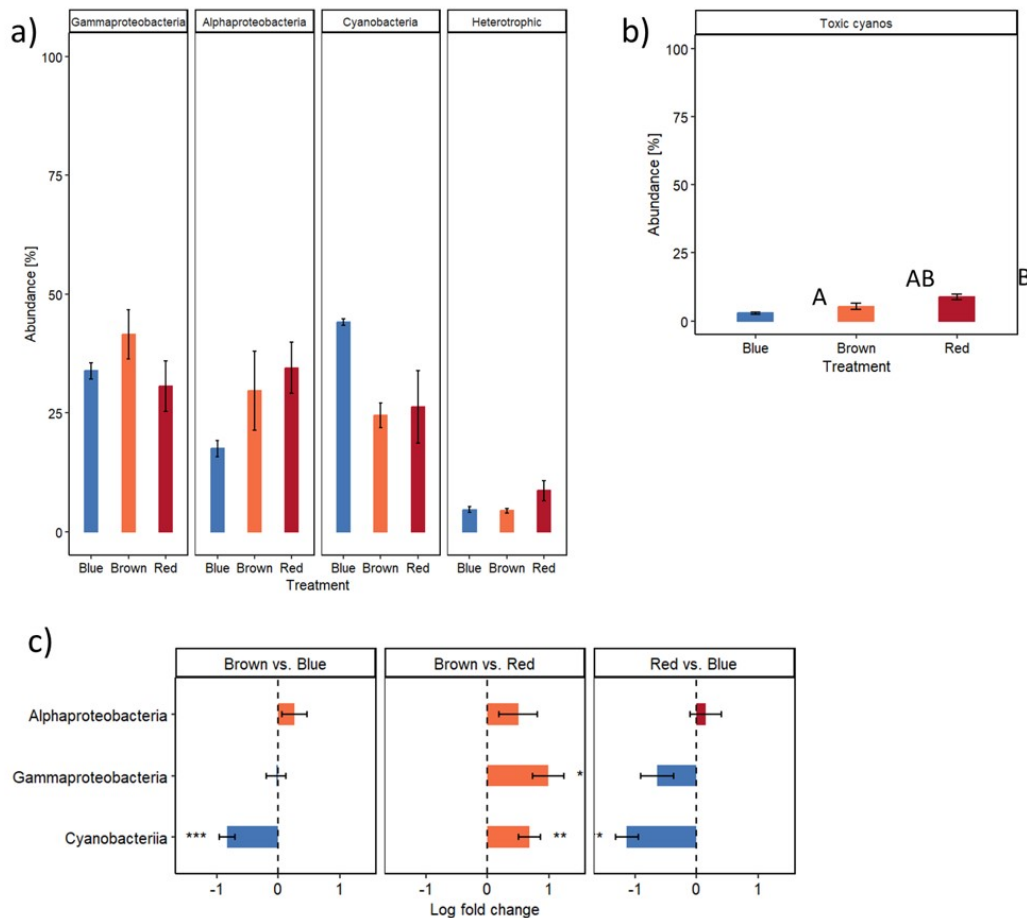


Figure 10. Relative abundances of bacterial taxa from the Kattegat after light incubation. Taxa grouped by photosynthetic potential (a), percentage of cyanobacteria which are potentially toxic (b), taxa which differed significantly after incubation as identified by ANCOM-BC analysis (c). Data are means and standard errors. Different letters indicate significant differences, where present, ($P < 0.05$) determined by Tukey's test.

after all treatments was Chl-*c* (>99%) (Figure 9b).

4. Discussion

Baltic Sea waters are optically complex and are classed as Case 2 waters due to high CDOM content (Levin et al., 2013). Water in the Baltic Proper can be predominantly green due to strong absorption of blue and red wavelengths, an effect which increases with depth (Haverkamp et al., 2008; Levin et al., 2013). We found higher proportions of green light at our Gotland Basin and Bothnian Bay sites than the Kattegat site (Figure 2, Supplementary Figure 1b). Both phytoplankton and CDOM contribute substantially to total light absorption in Baltic surface waters (Kratzer and Tett, 2009; Meler, Ostrowska and Stoń-Egiert, 2016) and the relationship between Chl-*a* and biomass is influenced by cell size, accessory pigment composition, and PAR availability which can vary seasonally (Meler et al., 2018).

These spatial differences in spectral composition create heterogeneous light environments across the Baltic

Sea within which phytoplankton communities may exhibit regional adaptation.

As expected, the initial communities differed among sites and were consistent with previous observations and monitoring data for the Baltic Sea. Salinity is the primary large-scale environmental gradient structuring pelagic communities in the Baltic Sea and likely contributed to the differences in initial community composition among basins (Hu et al., 2016). In the present experiment, salinity was not manipulated. Thus, the observed responses to spectral light treatments reflect community level adjustments within salinity conditioned assemblages. Greater proportions of mixotrophic cryptophytes and green algae were found in the Bothnian Bay compared to the Kattegat, while dinoflagellates and diatoms were most abundant in the Kattegat samples (Ojaveer et al., 2010; Hu et al., 2016). Picophytoplankton are associated with low light conditions like that of the Bothnian Bay because smaller cells are less affected by self-shading. The Bothnian Bay samples had the smallest proportions of cyanobacteria, in line with

studies of the northern Baltic, (Andersson et al., 2015), whereas the Gotland Basin samples had high proportions of *Telonemia*, as previously noted in the Baltic Proper (Hu et al., 2016). Species of the picocyanobacteria *Synechococcus* are known to differ across Baltic regions, and a divide was also seen here (Haverkamp et al., 2008; Haverkamp et al., 2009). Sequences from the Bothnian Bay and Gotland Basin clustered more closely with *S. lacustris*, associated with freshwater (Cabello-Yeves et al., 2022), whereas the Kattegat samples clustered closely to the CC9311 and CC9902 strains of *Synechococcus*, described as chromatic acclimators, capable of surviving in shifting spectral light environments (Larsson et al., 2014). This may be a result of the low salinity in the Baltic, and these strains are likely to be locally adapted so that we cannot describe their pigmentation status from these data.

The light treatments caused shifts in the eukaryotic and bacterial communities, demonstrating that spectral quality can restructure phytoplankton assemblages. Across basins, red light promoted heterotrophic eukaryotes, while phototrophs were at the highest relative abundances in blue light. Phototrophic cyanobacteria proportions were also higher in the blue light treatments and lower in red. In the Bothnian Bay samples, mixotroph proportions increased under red relative to blue light, whereas in the Gotland Basin heterotroph proportions were high after all treatments. These differences among sites suggest that responses to spectral shifts depend partly on pre-existing community structure and regional adaptation. Light intensity was low in all treatments so that phototrophs must efficiently use the available wavelengths. In the Gotland Basin samples, the treatments may have been limiting to phototrophic taxa. The Bothnian Bay samples showed that green algae, mainly *Bathycoccus* spp., although proportionally low overall, survived better in the limiting red and brown light treatments compared to green algae at the other sites. The differences among the samples sourced from the sites is likely due to existing adaptation in the responses of taxa in communities from the different regions.

Light absorption by phytoplankton differs depending on pigment composition (Meler et al., 2018), and grouping taxa by major accessory pigments revealed differences according to light treatment. In the Bothnian Bay, green algae containing Chl-*b* were most prevalent in blue light. Chl-*b* improves absorption of blue wavelengths (Lichtenhaler, 1987; Croce and van Amerongen, 2014). Taxa with both Chl-*c* and phycobiliproteins were most prevalent in red. In all sites, taxa with Chl-*c* remained prevalent after all light treatments. This suggests that the broader absorption range of Chl-*c* is advantageous in varying spectral conditions. Cryptophytes, which use chlorophylls *a* and *c*, and modify concentrations and structure of phycobiliproteins during photoacclimation (Heidenreich and Richardson, 2020; Spangler et al., 2022), also showed flexibility across treatments. Our results are in line with a previ-

ous study reporting that cryptophytes show positive responses to browning in lake experiments (Lyche Solheim et al., 2024). These results indicate that phytoplankton taxa with broader or more adaptable pigment systems may be favoured under the spectrally shifted light environments associated with increasing browning.

Changes in light quality influenced the relative dominance of functional groups but did not induce relative increases in taxa which are considered invasive or with potential for toxicity in the Baltic Sea. This suggests that light quality is not a driver for these concerns. Similarly, no consistent decrease in diatoms was seen in this study as a result of the light treatments. The filamentous cyanobacteria *Nodularia* was absent from the Bothnian Bay site and was most abundant in the Kattegat site, consistent with previous reports, (Olofsson et al., 2020). This genus persisted across light treatments, suggesting that light quality does not regulate its proliferation.

Heterotrophic bacteria were most prevalent at the Bothnian Bay site. Although Alphaproteobacteria and Gammaproteobacteria, contain proteorhodopsin which can absorb blue or green light (Slamovits et al., 2011), our abundance data do not indicate an advantage for this trait. An increase in mixotrophic phytoplankton has been observed along the south to north gradient in the Baltic (Paczkowska et al., 2017), and our results indicate that browning, red-shifted spectra may further favour mixotrophic and heterotrophic strategies relative to primarily phototrophic taxa.

5. Conclusion

Availability of light affects the comparative survival of phytoplankton species in a community. Heterotrophic eukaryote proportions were highest in red light, whereas diatom and other phototroph proportions were highest in blue light. In the Bothnian Bay, chlorophyte taxa which produce Chl-*b* were in higher proportions after blue light incubation, while red light samples had the highest proportion of cryptophyte taxa with Chl-*c* and phycobilins. Cyanobacteria proportions similarly decreased in red light and were highest in blue. These differences among sites likely reflect adaptation to light regimes along the Baltic gradient. Our study supports the hypothesis that spectral light quality is a hidden diversity driver, and that local adaptations to light spectrum occur.

Acknowledgement

We thank the crews of *r/v Svea* and *KBV181* for hosting and their assistance with sampling. We also thank the Swedish Agency for Marine and Water Management (Havsvattenmyndigheten) and SMHI for published data on the physiochemical characteristics of sites.

Funding

This study was financed by the Swedish Research Environment EcoChange, by the Gunnar and Ruth Björkman Fund, by the Swedish Agency for Marine and Water Management and the Swedish Environmental Protection Agency under the grant number NV-03728-17 and by the Swedish FOR-MAS (FR-2019/0007).

Author contributions

Funding acquisition, project administration, and conceptualisation by AA and ES informed by existing light quality data from UB. Investigation, methodology, data curation, formal analysis, visualisation, and writing original draft by ES, writing review and editing by ES and AA with advice from BK, AFA, and KTJ.

Supplementary material

Supplementary material associated with this article can be found [here](#).

Conflict of interest

None declared.

References

Allen, J.G., Siegel, D.A., Nelson, N.B., Halewood, S., 2020. *Controls on Ocean Color Spectra Observed During the North Atlantic Aerosols and Marine Ecosystems Study (NAAMES)*. *Front. Mar. Sci.* 7, 567007. <https://doi.org/10.3389/fmars.2020.567007>

Andersson, A., Falk, S., Samuelsson, G., Hagström, A., 1989. *Nutritional characteristics of a mixotrophic nanoflagellate, Ochromonas sp.* *Microb. Ecol.* 17 (3), 251–262. <https://doi.org/10.1007/BF02012838>

Andersson, A., Högländer, H., Karlsson, C., Huseby, S., 2015. *Key role of phosphorus and nitrogen in regulating cyanobacterial community composition in the northern Baltic Sea*. *Estuar. Coast. Shelf Sci.* 164, 161–171. <https://doi.org/10.1016/j.ecss.2015.07.013>

Ask, J., Rowe, O., Brugel, S., Strömgren, M., Byström, P., Andersson, A., 2016. *Importance of coastal primary production in the northern Baltic Sea*. *Ambio*, 45 (6), 635–648. <https://doi.org/10.1007/s13280-016-0778-5>

Balzano, S., Abs, E., Leterme, S.C., 2015. *Protist diversity along a salinity gradient in a coastal lagoon*. *Aquat. Microb. Ecol.* 74 (3), 263–277. <https://doi.org/10.3354/ame01740>

Biggs, T.E.G., Rozema, P.D., Evans, C., Timmermans, K.R., Meredith, M.P., Pond, D.W., Brussaard, C.P.D., 2022. *Control of Antarctic phytoplankton community composition and standing stock by light availability*. *Polar Biol.* 45, 1635–1653. <https://doi.org/10.1007/s00300-022-03094-5>

Bokulich, N.A., Kaehler, B.D., Rideout, J.R., Dillon, M., Bolyen, E., Knight, R., Huttley, G.A., Gregory Caporaso, J., 2018. *Optimizing taxonomic classification of marker-gene amplicon sequences with QIIME 2's q2-feature-classifier plugin*. *Microbiome*, 6 (1), 90. <https://doi.org/10.1186/s40168-018-0470-z>

Bolyen, E., Rideout, J.R., Dillon, M.R., et al., 2019. *Reproducible, interactive, scalable and extensible microbiome data science using QIIME 2*. *Nat. Biotechnol.* 37 (8), 852–857. <https://doi.org/10.1038/s41587-019-0209-9>

Båmstedt, U., 2019. *Comparing static and dynamic incubations in primary production measurements under different euphotic and mixing depths*. *Hydrobiologia*, 827 (1), 155–169. <https://doi.org/10.1007/s10750-018-3762-1>

Båmstedt, U., Wikner, J., 2016. *Mixing depth and allochthonous dissolved organic carbon: controlling factors of coastal trophic balance*. *Mar. Ecol. Prog. Ser.* 561, 17–29. <https://doi.org/10.3354/meps11907>

Cabello-Yeves, P.J., Callieri, C., Picazo, A., Schallenberg, L., Huber, P., Roda-Garcia, J.J., Bartosiewicz, M., Belykh, O.I., Tikhonova, I.V., Torcello-Requena, A., De Prado, P.M., Puxty, R.J., Millard, A.D., Camacho, A., Rodriguez-Valera, F., Scanlan, D.J., 2022. *Elucidating the picocyanobacteria salinity divide through ecogenomics of new freshwater isolates*. *BMC Biol.* 20 (1), 175. <https://doi.org/10.1186/s12915-022-01379-z>

Croce, R., van Amerongen, H., 2014. *Natural strategies for photosynthetic light harvesting*. *Nat. Chem. Biol.* 10 (7), 492–501. <https://doi.org/10.1038/nchembio.1555>

De Coster, W., Rademakers, R., 2023. *NanoPack2: population-scale evaluation of long-read sequencing data*. *Bioinformatics*, 39 (5), btad311. <https://doi.org/10.1093/bioinformatics/btad311>

Demir-Hilton, E., Sudek, S., Cuvelier, M.L., Gentemann, C.L., Zehr, J.P., Worden, A.Z., 2011. *Global distribution patterns of distinct clades of the photosynthetic picoeukaryote *Ostreococcus**. *ISME J.* 5 (7), 1095–107. <https://doi.org/10.1038/ismej.2010.209>

Edwards, K.F., Litchman, E., Klausmeier, C.A., 2013. *Functional traits explain phytoplankton community structure and seasonal dynamics in a marine ecosystem*. *Ecol. Lett.* 16 (1), 56–63. <https://doi.org/10.1111/ele.12012>

Figuroa, D., Rowe, O.F., Paczkowska, J., Legrand, C., Andersson, A., 2016. *Allochthonous Carbon-a Major Driver of Bacterioplankton Production in the Subarctic Northern Baltic Sea*. *Microb. Ecol.* 71 (4), 789–801. <https://doi.org/10.1007/s00248-015-0714-4>

Fortunato, A.F., Jaubert, M., Enomoto, G., Bouly, J.P., Raniello, R., Thaler, M., Malviya, S., Bernardes, J. S., Rappaport,

- 712 F., Gentili, B., Huysman, M.J., Carbone, A., Bowler, C.,
713 d'Alcalà, M.R., Ikeuchi, M., Falciatore, A., 2016. *Diatom*
714 *Phytochromes Reveal the Existence of Far-Red-Light-*
715 *Based Sensing in the Ocean*. *The Plant Cell*, 28 (3),
716 616–628.
717 <https://doi.org/10.1105/tpc.15.00928>
- 718 Guillou, L., Bachar, D., Audic, S., Bass, D., Berney, C., Bittner,
719 L., Boutte, C., Burgaud, G., de Vargas, C., Decelle, J., del
720 Campo, J., Dolan, J.R., Dunthorn, M., Edvardsen, B., Holz-
721 mann, M., Kooistra, W.H.C.F., Lara, E., Le Bescot, N., Log-
722 ares, R., Mahé, F., Massana, R., Montresor, M., Morard,
723 R., Not, F., Pawlowski, J., Probert, I., Sauvadet, A.-L.,
724 Siano, R., Stoeck, T., Vaulot, D., Zimmermann, P., Chris-
725 ten, R., 2013. *The Protist Ribosomal Reference database*
726 *(PR2): a catalog of unicellular eukaryote Small Sub-Unit*
727 *rRNA sequences with curated taxonomy*. *Nucleic Acids*
728 *Res.* 41 (D1), D597–D604.
729 <https://doi.org/10.1093/nar/gks1160>
- 730 Harvey, E.T., Kratzer, S., Andersson, A., 2015. *Relation-*
731 *ships between colored dissolved organic matter and*
732 *dissolved organic carbon in different coastal gradients*
733 *of the Baltic Sea*. *Ambio*, 44 (Suppl. 3), 392–401.
734 <https://doi.org/10.1007/s13280-015-0658-4>
- 735 Haverkamp, T., Acinas, S.G., Doeleman, M., Stomp, M., Huis-
736 man, J., Stal, L.J., 2008. *Diversity and phylogeny of*
737 *Baltic Sea picocyanobacteria inferred from their ITS*
738 *and phycobiliprotein operons*. *Environ. Microbiol.* 10
739 (1), 174–188.
740 <https://doi.org/10.1111/j.1462-2920.2007.01442.x>
- 741 Haverkamp, T.H., Schouten, D., Doeleman, M., Wollenzien,
742 U., Huisman, J., Stal, L.J., 2009. *Colorful microdiversity*
743 *of Synechococcus strains (picocyanobacteria) isolated*
744 *from the Baltic Sea*. *ISME J.* 3 (4), 397–408.
745 <https://doi.org/10.1038/ismej.2008.118>
- 746 Heidenreich, K.M., Richardson, T.L., 2020. *Photopigment,*
747 *Absorption, and Growth Responses of Marine Crypto-*
748 *phytes to Varying Spectral Irradiance* *J. Phycol.* 56 (2),
749 507–520.
750 <https://doi.org/10.1111/jpy.12962>
- 751 Hill, J., Enbody, E.D., Pettersson, M.E., Sprehn, C.G., Bekkevold,
752 D., Folkvord, A., Laikre, L., Kleinau, G., Scheerer, P., An-
753 dersson, L., 2019. *Recurrent convergent evolution at*
754 *amino acid residue 261 in fish rhodopsin*. *Proc. Natl.*
755 *Acad. Sci. USA*, 116 (37), 18473–18478.
756 <https://doi.org/10.1073/pnas.1908332116>
- 757 Hu, Y.O., Karlson, B., Charvet, S., Andersson, A.F., 2016. *Di-*
758 *versity of Pico- to Mesoplankton along the 2000 km*
759 *Salinity Gradient of the Baltic Sea*. *Front. Microbiol.* 7,
760 679.
761 <https://doi.org/10.3389/fmicb.2016.00679>
- 762 Hugerth, L.W., Muller, E.E., Hu, Y.O., Lebrun, L.A., Roume, H.,
763 Lundin, D., Wilmes, P., Andersson, A.F., 2014. *System-*
764 *atic design of 18S rRNA gene primers for determining*
765 *eukaryotic diversity in microbial consortia*. *PLoS One*,
766 9 (4), e95567.
<https://doi.org/10.1371/journal.pone.0095567>
- 767 Johnsen, G., Sakshaug, E., Vernet, M., 1992. *Pigment com-*
768 *position, spectral characterization and photosynthetic*
769 *parameters in Chrysochromulina polylepis*. *Mar. Ecol.*
770 *Prog. Ser.* 83 (2/3), 241–249.
771
- 772 Kehoe, D.M., Grossman, A.R., 1994. *Complementary chro-*
773 *matic adaptation: photoperception to gene regulation*.
774 *Semin. Cell. Biol.* 5 (5), 303–313.
775 <https://doi.org/10.1006/scel.1994.1037>
- 776 Kratzer, S., Moore, G., 2018. *Inherent Optical Properties of*
777 *the Baltic Sea in Comparison to Other Seas and Oceans*.
778 *Remote Sens.* 10 (3), 418.
779 <https://doi.org/10.3390/rs10030418>
- 780 Kratzer, S., Tett, P., 2009. *Using bio-optics to investigate the*
781 *extent of coastal waters: A Swedish case study*. *Hydro-*
782 *biologia*, 629 (1), 169–186.
783 <https://doi.org/10.1007/s10750-009-9769-x>
- 784 Krehenwinkel, H., Pomerantz, A., Henderson, J.B., Kennedy,
785 S.R., Lim, J.Y., Swamy, V., Shoobridge, J.D., Graham, N.,
786 Patel, N.H., Gillespie, R.G., Prost, S., 2019. *Nanopore*
787 *sequencing of long ribosomal DNA amplicons enables*
788 *portable and simple biodiversity assessments with high*
789 *phylogenetic resolution across broad taxonomic scale*.
790 *Gigascience*, 8 (5), giz006.
791 <https://doi.org/10.1093/gigascience/giz006>
- 792 Larsson, J., Celepli, N., Ininbergs, K., Dupont, C.L., Yooseph,
793 S., Bergman, B., Ekman, M., 2014. *Picocyanobacteria*
794 *containing a novel pigment gene cluster dominate the*
795 *brackish water Baltic Sea*. *ISME J.* 8 (9), 1892–903.
796 <https://doi.org/10.1038/ismej.2014.35>
- 797 Latz, M.A.C., Grujic, V., Brugel, S., Lycken, J., John, U., Karl-
798 son, B., Andersson, A., Andersson, A.F., 2022. *Short-*
799 *and long-read metabarcoding of the eukaryotic rRNA*
800 *operon: Evaluation of primers and comparison to shot-*
801 *gun metagenomics sequencing*. *Mol. Ecol. Resour.* 22
802 (6), 2304–2318.
803 <https://doi.org/10.1111/1755-0998.13623>
- 804 Levin, I., Darecki, M., Sagan, S., Radomyslskaya, T., 2013.
805 *Relationships between inherent optical properties in the*
806 *Baltic Sea for application to the underwater imaging*
807 *problem*. *Oceanologia*, 55 (1), 11–26.
808 <https://doi.org/10.5697/oc.55-1.011>
- 809 Lichtenthaler, H., 1987. *Chlorophyll and carotenoids: Pig-*
810 *ments of photosynthetic biomembranes*. *Methods En-*
811 *zymol.* 148, 331–382.
812 [https://doi.org/10.1016/0076-6879\(87\)48036-1](https://doi.org/10.1016/0076-6879(87)48036-1)
- 813 Lin, H., Peddada, S.D., 2020. *Analysis of compositions of*
814 *microbiomes with bias correction*. *Nat. Commun.* 11
815 (1), 3514.
816 <https://doi.org/10.1038/s41467-020-17041-7>
- 817 Luimstra, V.M., Verspagen, J.M.H., Xu, T., Schuurmans, J.M.,
818 Huisman, J., 2020. *Changes in water color shift compe-*
819 *tition between phytoplankton species with contrasting*
820 *light-harvesting strategies*. *Ecology*, 101 (3), e02951.

- 821 Lyche Solheim, A., Gundersen, H., Mischke, U., Skjelbred,
822 B., Nejtgaard, J.C., Guislain, A.L.N., Sperfeld, E., Giling,
823 D.P., Haande, S., Ballot, A., Moe, S.J., Stephan, S., Walles,
824 T.J.W., Jechow, A., Minguez, L., Ganzert, L., Hornick, T.,
825 Hansson, T.H., Stratmann, C.N., Järvinen, M., Drakare, S.,
826 Carvalho, L., Grossart, H.-P., Gessner, M. O. and Berger,
827 S.A., 2024. *Lake browning counteracts cyanobacteria*
828 *responses to nutrients: Evidence from phytoplankton*
829 *dynamics in large enclosure experiments and compre-*
830 *hensive observational data.* *Glob.Change Biol.* 30 (1),
831 e17013.
832 <https://doi.org/10.1111/gcb.17013>
- 833 McDonald, D., Jiang, Y., Balaban, M., Cantrell, K., Zhu, Q., Gon-
834 zalez, A., Morton, J.T., Nicolaou, G., Parks, D.H., Karst,
835 S.M., Albertsen, M., Hugenholtz, P., DeSantis, T., Song,
836 S.J., Bartko, A., Havulinna, A.S., Jousilahti, P., Cheng, S.,
837 Inouye, M., Niiranen, T., Jain, M., Salomaa, V., Lahti, L.,
838 Mirarab, S., Knight, R., 2023. *Greengenes2 unifies mi-*
839 *crobial data in a single reference tree.* *Nat. Biotechnol.*
840 42, 715–718.
841 <https://doi.org/10.1038/s41587-023-01845-1>
- 842 Meler, J., Ostrowska, M., Stoń-Egiert, J., 2016. *Seasonal*
843 *and spatial variability of phytoplankton and non-algal*
844 *absorption in the surface layer of the Baltic.* *Estuar.*
845 *Coast. Shelf Sci.* 180, 123–135.
- 846 Meler, J., Woźniak, S.B., Stoń-Egiert, J., Woźniak, B., 2018.
847 *Parameterization of phytoplankton spectral absorption*
848 *coefficients in the Baltic Sea: general, monthly and two-*
849 *component variants of approximation formulas.* *Ocean*
850 *Sci.* 14 (6), 1523–1545.
851 <https://doi.org/10.5194/os-14-1523-2018>
- 852 Modis, N.A., 2022. *Moderate-resolution Imaging Spectroradi-*
853 *ometer (MODIS) AQUA Level-3 Mapped Inherent Opti-*
854 *cal Properties. Version 2022.* (Accessed: 06/05/2023).
- 855 Neun, S., Hintz, N.H., Schröder, M., Striebel, M., 2022. *Phy-*
856 *toplankton Response to Different Light Colors and Fluc-*
857 *tuation Frequencies.* *Front. Mar. Sci.* 9, 824624.
858 <https://doi.org/10.3389/fmars.2022.824624>
- 859 Ojaveer, H., Jaanus, A., MacKenzie, B.R., Martin, G., Olenin,
860 S., Radziejewska, T., Telesh, I., Zettler, M.L., Zaiko, A.,
861 2010. *Status of Biodiversity in the Baltic Sea.* *PLOS One*,
862 5 (9), e12467.
863 <https://doi.org/10.1371/journal.pone.0012467>
- 864 Olenina, I., Hajdu, S., Edler, L., Andersson, A., Wasmund, N.,
865 Göbel, J., Huttunen, M., Jaanus, A., Ledaine, I., Huseby,
866 S., Niemkiewicz, E., 2006. *Biovolumes and size-classes*
867 *of phytoplankton in the Baltic Sea.* *Dept. Eco. Environ.*
868 *Sci., Umeå Marine Sciences Centre (UMF), available at:*
869 <https://epic.awi.de/id/eprint/30141/1/bsep106.pdf>
- 870 Olofsson, M., Suikkanen, S., Kobos, J., Wasmund, N., Karl-
871 son, B., 2020. *Basin-specific changes in filamentous*
872 *cyanobacteria community composition across four decades*
873 *in the Baltic Sea.* *Harmful Algae*, 91, 101685.
874 [10.1016/j.hal.2019.101685](https://doi.org/10.1016/j.hal.2019.101685)
- Paczkowska, J., Rowe, O.F., Schlüter, L., Legrand, C., Karlson,
875 B., Andersson, A., 2017. *Allochthonous matter: an im-*
876 *portant factor shaping the phytoplankton community*
877 *in the Baltic Sea.* *J. Plankton Res.* 39 (1), 23–34.
878 <https://doi.org/10.1093/plankt/fbw081>
- 879 Palenik, B., 2001. *Chromatic adaptation in marine Syne-*
880 *chococcus strains.* *Appl. Environ. Microbiol.* 67(2),
881 991–994.
882 <https://doi.org/10.1128/AEM.67.2.991-994.2001>
- 883 Rognes, T., Flouri, T., Nichols, B., Quince, C., Mahé, F., 2016.
884 *VSEARCH: a versatile open source tool for metagenomics.*
885 *Peer J.* 4, e2584.
886 <https://doi.org/10.7717/peerj.2584>
- 887 Roy, S., Llewellyn, C.A., Egeland, E.S., Johnsen, G., 2011.
888 *Phytoplankton Pigments: Characterization, Chemotax-*
889 *onomy and Applications in Oceanography.* Cambridge
890 University Press.
- 891 Sakshaug, E., Slagstad, D., 1991. *Light and productivity of*
892 *phytoplankton in polar marine ecosystems: a physiolog-*
893 *ical view.* *Polar Res.* 10 (1), 69–86.
894 <https://doi.org/10.3402/polar.v10i1.6729>
- 895 Sands, E., Davies, S., Puxty, R.J., Vergé, V., Bouget, F.Y., Scan-
896 lan, D.J., Carré, I.A., 2023. *Genetic and physiological*
897 *responses to light quality in a deep ocean ecotype of*
898 *Ostreococcus, an ecologically important photosynthetic*
899 *picoeukaryote.* *J. Exp. Bot.* 74 (21), 6773–6789.
900 <https://doi.org/10.1093/jxb/erad347>
- 901 Santos, A., van Aarle, R., Barrientos, L., Martinez-Urtaza,
902 J., 2020. *Computational methods for 16S metabarcod-*
903 *ing studies using Nanopore sequencing data.* *Comput.*
904 *Struct. Biotechnol. J.* 18, 296–305.
905 <https://doi.org/10.1016/j.csbj.2020.01.005>
- 906 Senar, O.E., Creed, I.F., Trick, C.G., 2021. *Lake browning may*
907 *fuel phytoplankton biomass and trigger shifts in phyto-*
908 *plankton communities in temperate lakes.* *Aquatic Sci.*
909 83 (2), 21.
910 <https://doi.org/10.1007/s00027-021-00780-0>
- 911 Simis, S.G., Ylöstalo, P., Kallio, K.Y., Spilling, K., Kutser, T.,
912 2017. *Contrasting seasonality in optical-biogeochemical*
913 *properties of the Baltic Sea.* *PLoS One*, 12 (4), e0173357.
914 <https://doi.org/10.1371/journal.pone.0173357>
- 915 Slamovits, C.H., Okamoto, N., Burri, L., James, E.R., Keeling,
916 P.J., 2011. *A bacterial proteorhodopsin proton pump in*
917 *marine eukaryotes.* *Nat. Commun.* 2 (1), 183.
918 <https://doi.org/10.1038/ncomms1188>
- 919 SMHI, 2023. *SHARK – Regional marine environmental moni-*
920 *toring and monitoring projects of Epibenthos in Sweden*
921 *since 1994,* (Accessed: 06/05/2024).
- 922 Spangler, L.C., Yu, M., Jeffrey, P.D., Scholes, G.D., 2022. *Con-*
923 *trollable Phycobilin Modification: An Alternative Pho-*
924 *toacclimation Response in Cryptophyte Algae.* *ACS Cent.*
925 *Sci.* 8 (3), 340–350.
926 <https://doi.org/10.1021/acscentsci.1c01209>
- 927 Spilling, K., Asmala, E., Haavisto, N., Haraguchi, L., Kraft, K.,
928 Lehto, A.M., Lewandowska, A.M., Norkko, J., Piiparinen,
929

- 930 J., Seppälä, J., Vanharanta, M., Vehmaa, A., Ylöstalo, P.,
931 Tamminen, T., 2022. *Brownification affects phytoplankton*
932 *community composition but not primary productivity*
933 *in eutrophic coastal waters: A mesocosm experiment*
934 *in the Baltic Sea*. *Sci. Total. Environ.* 841, 156510.
935 <https://doi.org/10.1016/j.scitotenv.2022.156510>
- 936 Stomp, M., Huisman, J., De Jongh, F., Veraart, A.J., Gerla, D.,
937 Rijkeboer, M., Ibelings, B.W., Wollenzien, U.I., Stal, L.J.,
938 2004. *Adaptive divergence in pigment composition pro-*
939 *motes phytoplankton biodiversity*. *Nature*, 432 (7013),
940 104–107.
941 <https://doi.org/10.1038/nature03044>
- 942 Stomp, M., Huisman, J., Stal, L.J., Matthijs, H.C., 2007. *Color-*
943 *ful niches of phototrophic microorganisms shaped by vi-*
944 *brations of the water molecule*. *ISME J.* 1 (4), 271–282.
945 <https://doi.org/10.1038/ismej.2007.59>
- 946 Strååt, K.D., Mörth, C.-M., Undeman, E., 2018. *Future export*
947 *of particulate and dissolved organic carbon from land*
948 *to coastal zones of the Baltic Sea*. *J. Marine Syst.* 177,
949 8–20.
950 <https://doi.org/10.1016/j.jmarsys.2017.09.002>
- 951 Škerlep, M., Nehzati, S., Johansson, U., Kleja, D.B., Persson,
952 P., Kritzberg, E.S., 2022. *Spruce forest afforestation*
953 *leading to increased Fe mobilization from soils*. *Biogeo-*
954 *chemistry*, 157 (3), 273–290.
955 <https://doi.org/10.1007/s10533-021-00874-9>
- 956 Valle, K.C., Nymark, M., Aamot, I., Hancke, K., Winge, P., An-
957 dresen, K., Johnsen, G., Brembu, T., Bones, A.M., 2014.
958 *System responses to equal doses of photosynthetically*
959 *usable radiation of blue, green, and red light in the ma-*
960 *rine diatom Phaeodactylum tricorutum*. *PLoS One*, 9
961 (12), e114211.
962 <https://doi.org/10.1371/journal.pone.0114211>
- 963 Wasmund, N., Uhlig, S., 2003. *Phytoplankton trends in the*
964 *Baltic Sea*. *ICES J. Mar. Sci.* 60 (2), 177–186.
965 [https://doi.org/10.1016/S1054-3139\(02\)00280-1](https://doi.org/10.1016/S1054-3139(02)00280-1)
- 966 Werdell, P.J., McKinna, L.I.W., Boss, E., Ackleson, S.G., Craig,
967 S.E., Gregg, W.W., Lee, Z., Maritorena, S., Roesler, C.S.,
968 Rousseaux, C.S., Stramski, D., Sullivan, J.M., Twardowski,
969 M.S., Tzortziou, M., Zhang, X., 2018. *An overview of*
970 *approaches and challenges for retrieving marine inher-*
971 *ent optical properties from ocean color remote sensing*.
972 *Prog. Oceanogr.* 160, 186–212.
973 <https://doi.org/10.1016/j.pocean.2018.01.001>
- 974 Xiao, Y., Rohrlack, T., Riise, G., 2020. *Unraveling long-term*
975 *changes in lake color based on optical properties of lake*
976 *sediment*. *Sci. Total. Environ.* 699, 134388.
977 <https://doi.org/10.1016/j.scitotenv.2019.134388>